⌘ *Author's Choice*

THE JOURNAL OF BIOLOGICAL CHEMISTRY VOL. 285, NO. 10, pp. 7016–7027, March 5, 2010

Mycobacterium tuberculosis cAMP Receptor Protein (Rv3676) Differs from the *Escherichia coli* Paradigm in Its cAMP Binding and DNA Binding Properties and Transcription Activation Properties*[S]

Received for publication, July 22, 2009, and in revised form, November 18, 2009 Published, JBC Papers in Press, December 22, 2009, DOI 10.1074/jbc.M109.047720

Melanie Stapleton[‡], Ihtshamul Haq[§], Debbie M. Hunt[¶], Kristine B. Arnvig[¶], Peter J. Artymiuk[‡], Roger S. Buxton[¶], and Jeffrey Green[‡1]

From the [‡]Department of Molecular Biology and Biotechnology, University of Sheffield, Sheffield, S10 2TN, the [§]Department of Chemistry, University of Sheffield, Sheffield S3 7HF, and the [¶]Division of Mycobacterial Research, Medical Research Council National Institute for Medical Research, Mill Hill, London NW7 1AA, United Kingdom

The pathogen *Mycobacterium tuberculosis* produces a burst of cAMP upon infection of macrophages. Bacterial cyclic AMP receptor proteins (CRP) are transcription factors that respond to cAMP by binding at target promoters when cAMP concentrations increase. Rv3676 (CRP^{Mt}) is a CRP family protein that regulates expression of genes (*rpfA* and *whiB1*) that are potentially involved in *M. tuberculosis* persistence and/or emergence from the dormant state. Here, the CRP^{Mt} homodimer is shown to bind two molecules of cAMP (one per protomer) at noninteracting sites. Furthermore, cAMP binding by CRP^{Mt} was relatively weak, entropy driven, and resulted in a relatively small enhancement in DNA binding. Tandem CRP^{Mt}-binding sites (CRP1 at −58.5 and CRP2 at −37.5) were identified at the *whiB1* promoter (P*whiB1*). *In vitro* transcription reactions showed that CRP1 is an activating site and that CRP2, which was only occupied in the presence of cAMP or at high CRP^{Mt} concentrations in the absence of cAMP, is a repressing site. Binding of CRP^{Mt} to CRP1 was not essential for open complex formation but was required for transcription activation. Thus, these data suggest that binding of CRP^{Mt} to the P*whiB1* CRP1 site activates transcription at a step after open complex formation. In contrast, high cAMP concentrations allowed occupation of both CRP1 and CRP2 sites, resulting in inhibition of open complex formation. Thus, *M. tuberculosis* CRP has evolved several distinct characteristics, compared with the *Escherichia coli* CRP paradigm, to allow it to regulate gene expression against a background of high concentrations of cAMP.

Mycobacterium tuberculosis is one of the most successful human pathogens, contributing to the deaths of ~2 million people per annum by causing tuberculosis (1). It is an adaptable bacterium capable of survival in its preferred environment, the interior of a macrophage (2), and within droplet nuclei in the atmosphere that are produced by infected individuals. The disease is spread by inhalation of such droplets, and following initial infection, *M. tuberculosis* can persist in a nonreplicating state from which it may emerge when conditions are more favorable (*e.g.* when the immune system is suppressed), a phenomenon known as reactivation tuberculosis (3). This strategy has been so successful that the reservoir of infection is thought to be as great as one-third of the world's population (1), and thus the potential for reactivation tuberculosis is very large.

Appropriate gene regulation is likely to be vital for establishing and emerging from the dormant state. The presence of >100 regulator proteins, 11 two-component systems, 6 serine-threonine protein kinases, and 13 alternative σ factors (4) suggests that transcription regulation is important for *M. tuberculosis* pathogenesis. Cyclic AMP is likely to be an important signaling molecule in *M. tuberculosis* because it is predicted to possess 17 genes encoding adenylyl cyclases (4), at least one of which, Rv0386, is required for virulence (5). Interestingly, cAMP levels increase upon infection of macrophages by pathogenic mycobacteria (6, 7), and furthermore, addition of cAMP to cultures of *M. tuberculosis* causes changes in gene expression (8). Recently, Bishai and co-workers (5) showed that upon infection of macrophages, a bacterially derived cAMP burst promotes bacterial survival by interfering with host signaling pathways, but as well as influencing host regulatory networks, cAMP is also important in bacterial gene regulation.

The best characterized bacterial cAMP-responsive transcriptional regulator is the *Escherichia coli* cyclic AMP receptor protein (CRP,[2] sometimes known as catabolite gene activator protein). *E. coli* CRP is activated by binding cAMP and controls aspects of carbon metabolism and virulence gene expression and may act as a more general chromosome organizer (9–11). In *E. coli* under conditions of glucose starvation, intracellular cAMP concentrations increase via a mechanism involving interactions between the glucose phosphotransferase system transporter and adenylyl cyclase (12). Cyclic AMP is bound by the *E. coli* CRP dimer resulting in enhanced recognition of a specific DNA sequence (TGTGANNNNNNTCACA) present within the promoter regions of target genes (13). At activated promoters, CRP recruits RNA po-

* This work was supported by The Wellcome Trust Grant 078731/Z/05/Z and the Medical Research Council.

⌘ *Author's Choice*—Final version full access.

[S] The on-line version of this article (available at http://www.jbc.org) contains supplemental Figs. S1–S3.

[1] To whom correspondence should be addressed. Tel.: 44-144-222-4403; Fax: 44-144-222-2800; E-mail: jeff.green@sheffield.ac.uk.

[2] The abbreviations used are: CRP, cyclic AMP receptor protein; α-CTD, RNA polymerase α-subunit C-terminal domain; CRP^{Mt}, *M. tuberculosis* CRP protein encoded by the gene *Rv3676*; RNAP, RNA polymerase.

lymerase (RNAP) and promotes transcription by establishing specific protein-protein contacts (10, 14).

The *M. tuberculosis* Rv3676 protein (hereafter CRP^{Mt}) is a member of the CRP family (15–17). CRP^{Mt} is 32% identical (53% similar) over 189 amino acids to *E. coli* CRP (16). Like CRP in *E. coli*, CRP^{Mt} is a global transcriptional regulator because a deletion mutant has altered transcription of a large number of genes (16). Moreover, it is implicated in the virulence of *M. tuberculosis* because the CRP^{Mt} mutant is attenuated for growth in mice and macrophages as well as *in vitro* (16). Polymorphisms in CRP that enhance DNA binding have also occurred in the Bacillus Calmette-Guérin vaccine strain of *Mycobacterium bovis* (18–20) and result in changes in transcription of a number of genes, which, although not contributing to the attenuation of Bacillus Calmette-Guérin, may have been selected by growth *in vitro* (20).

In the CRP^{Mt} mutant, the largest decreases in expression were for the *rpfA* and *whiB1* genes (16). *In vivo* and *in vitro* analyses indicated that CRP^{Mt} activates expression of *rpfA* and *whiB1* (16, 17). These are potentially significant observations because *rpfA* encodes a protein that is thought to be involved in reviving dormant bacteria (21), and *whiB1* encodes a Wbl family protein (22). Wbl proteins are found only in actinomycetes and bind redox-sensitive iron-sulfur clusters (23, 24). The mechanism(s) of action of Wbl proteins is still unclear; some have been reported to have protein-disulfide reductase activity (24), and at least one (WhiB3) has been shown to bind DNA (25), consistent with the suggestion that Wbl proteins are transcription factors that might function in the control of developmental processes (22, 26). This latter suggestion raises the possibility that CRP^{Mt} in complex with cAMP regulates genes involved in the developmental switch associated with *M. tuberculosis* persistence and/or emergence from the dormant state. However, previous work suggested that although CRP^{Mt} binds cAMP, this interaction induces a relatively small enhancement in specific DNA binding (15–17). Thus, there are differences between *E. coli* CRP, where the presence of cAMP enhances specific DNA binding by several orders of magnitude (27), and CRP^{Mt}. Hence, the aim of this work was to investigate the interaction between CRP^{Mt} and cAMP and determine the mechanism of CRP^{Mt}-mediated activation of *whiB1* expression. Here, the following points are shown: (i) CRP^{Mt} dimer binds two molecules of cAMP; (ii) unlike *E. coli* CRP, the CRP^{Mt} cAMP-binding sites do not interact; (iii) CRP^{Mt} binds at two immediately adjacent sites in the *whiB1* promoter; and (iv) occupation of the upstream CRP^{Mt}-binding site at low cAMP concentrations activates *whiB1* transcription at a step after open complex formation, whereas occupation of the downstream site at high cAMP concentrations antagonizes activation from the upstream site by preventing open complex formation. In addition, a molecular model based on the *E. coli* CRP structure provides a plausible explanation for the distinctive cAMP binding properties of CRP^{Mt}.

EXPERIMENTAL PROCEDURES

Bacterial Strains, Plasmids, and Growth Conditions—Bacterial strains and plasmids are listed in Table 1. *E. coli* cultures were grown in Luria-Bertani (LB) medium (36) in a 1:5 volume/flask ratio at 37 °C with shaking at 250 rpm, except for *in vivo* transcription experiments where strains were grown in a 1:25 volume/flask ratio. Where required, antibiotics were added to media at the following concentrations: tetracycline 35 μg ml^{-1}, kanamycin 50 μg ml^{-1}, ampicillin 100 μg ml^{-1}. *M. tuberculosis* cultures (100 ml) were grown in 1 liter of polycarbonate culture bottles (Techmate) in a Bellco roll-in incubator (2 rpm) at 37 °C in Dubos broth containing 0.05% (v/v) Tween 80 supplemented with 0.2% (v/v) glycerol and 4% Dubos medium albumin. Where required, kanamycin was added at a final concentration of 25 μg ml^{-1}. *Mycobacterium smegmatis* was grown to log phase (56 h) in LB medium in a 1:5 volume/flask ratio at 37 °C with shaking at 250 rpm.

Overproduction and Purification of CRP^{Mt}—The CRP^{Mt} (Rv3676) open reading frame was amplified by PCR using primers Myc1746 (5′-CATCATGAATTCGTGGACGAGATCCTGGCC-3′) and Myc1747 (5′-CATCATACTCGAGCACTATTACCTCGCTCGGCGGGC-3′) containing engineered EcoRI and XhoI sites, respectively. This fragment was ligated into the corresponding sites of a pET28a derivative, in which the kanamycin resistance gene had been disrupted by the insertion of an ampicillin resistance gene (*bla*). The resulting plasmid (pGS2132) encoded a His_6-CRP^{Mt} fusion protein. The plasmid pGS2132 was moved into *E. coli* strain JRG5876 (BL21 λDE3 Δ*cyaA*), for expression of the recombinant protein by addition of 1 mM isopropyl 1-thio-β-D-galactopyranoside, followed by a further 3-h growth at 37 °C before collecting the bacteria by centrifugation. The bacteria were lysed by resuspending in 20 mM sodium phosphate, pH 7.2, containing 0.5 M NaCl, followed by repeated freeze-thawing and sonication. The lysate was cleared by centrifugation, and the resulting cell-free extract was passed through a nickel-charged Hi-Trap chelating column (GE Healthcare). The recombinant His_6-CRP^{Mt} protein was eluted using an imidazole gradient (0–500 mM in 20 ml). The pooled fractions containing His_6-CRP^{Mt} were dialyzed in phosphate-buffered saline (137 mM NaCl, 2.7 mM KCl, 10 mM Na_2HPO_4, 2 mM KH_2PO_4), and 10% (v/v) glycerol was added to the protein before storage at −20 °C. Where indicated the His_6 tag was removed by treatment with the protease thrombin (10 units for 16 h at 4 °C).

Trypsin Digestion of His_6-CRP^{Mt}—Recombinant His_6-CRP^{Mt} (15 μg) was incubated with 2 mM cAMP or cGMP for 10 min at 37 °C, followed by the addition of a second cyclic nucleotide (2 mM) for 10 min where indicated. The protein was then cleaved with 1 μg of trypsin (Sigma) for up to 10 min at 20 °C, and the reaction was stopped by the addition of 1.3% SDS and heating to 100 °C for 10 min. The resulting fragments were analyzed on a 15% SDS-polyacrylamide gel.

Isothermal Calorimetry—Recombinant His_6-CRP^{Mt} was extensively dialyzed against phosphate-buffered saline, and the concentration of protein was determined by SDS-PAGE and amino acid analysis (ion exchange chromatography and ninhydrin detection). The sodium salt of cAMP was dissolved in the dialysate phosphate-buffered saline, and the concentration was determined by UV absorption spectroscopy using the extinction coefficient of ϵ_{260} of 1.23×10^4 M^{-1} cm^{-1}. All samples were centrifuged prior to the titrations. The titration calorimetry measurements were performed using a MicroCal VP-ITC (MicroCal LLC, Northampton, MA). The isothermal calorim-

TABLE 1

Bacterial strains and plasmids

IPTG is isopropyl 1-thio-β -D -galactopyranoside.

Strain or plasmid	Relevant characteristics	Source or Ref.
***E. coli* strains**		
BL21 (λDE3)	Lysogen of λDE3 carrying a copy of the T7 RNAP under the control of the IPTG-inducible *lacUV5* promoter	Novagen
JRG5876	BL21 (λDE3) Δ*cyaA*; kan^R	This work
JRG6015	JRG5876 pGS2132	This work
M182	*E. coli* K12 Δ*lac*	28
JRG2630	M182 Δ *crp* derivative	29
JRG5875	M182 Δ*crp* Δ*cyaA*	This work
JRG6016	JRG2630 p2130 ptac85	This work
JRG6017	JRG2630 p2130 pGS1645	This work
JRG6018	JRG5875 p2130 ptac85	This work
JRG6019	JRG5875 p2130 pGS1645	This work
***M. tuberculosis* strains**		
H37Rv	Wild-type virulent strain	30
ΔRv3676	H37Rv, deletion of *Rv3676* (CRP^{Mt})	16
H37Rv/pRB142	H37Rv, with *whiB1-lacZ* reporter plasmid pRB142	This work
H37Rv/pRB143	H37Rv, with *whiB1-lacZ* reporter plasmid pRB143	This work
H37Rv/pRB144	H37Rv, with *whiB1-lacZ* reporter plasmid pRB144	This work
H37Rv/pRB145	H37Rv, with *whiB1-lacZ* reporter plasmid pRB145	This work
H37Rv/pRB146	H37Rv, with *whiB1-lacZ* reporter plasmid pRB146	This work
ΔRv3676/pRB142	ΔRv3676, with *whiB1-lacZ* reporter plasmid pRB142	This work
***M. smegmatis* strains**		
mc^2 155	Source of RNAP	31
***E. coli* plasmids**		
pCR4Blunt-TOPO	General cloning vector for blunt-ended PCR products; Ap^R, Kan^R	Invitrogen
pET28a	His$_6$ tag overexpression vector; Kan^R	Novagen
pRW50	*lacZ* transcriptional reporter plasmid; Tet^R	32
ptac85	Expression vector with an IPTG-inducible promoter; Ap^R	33
pGS1645	ptac85 containing *Rv3676* gene	This work
pGS2060	pCR4Blunt-TOPO containing the region upstream of *whiB1*	This work
p2130	pRW50 containing *CCgalΔ4*, a derivative of *galP1* with a consensus CRP-binding site centered at position −37.5 bp	34
pGS2132	pET28a derivative encoding His$_6$-CRP^{Mt} fusion protein; Ap^R	This work
pGS2060	pCR4Blunt-TOPO containing the 285-bp region upstream of *whiB1*	This work
pGS2061	As pGS2060 but with CRP^{Mt} site 1 altered to AGTTAGATAGCCAACG	This work
p2225	As pGS2060 but with CRP^{Mt} site 2 altered to CCAAACACTATTGACA	This work
p2227	As pGS2060 but with CRP^{Mt} site 1 and site 2 altered	This work
***M. tuberculosis* shuttle plasmids**		
pEJ414	*lacZ* transcriptional reporter plasmid; Kan^R	E. O. Davis (35)
pRB142	pEJ414 derivative containing transcriptional fusion of *whiB1* upstream region with *lacZ*	This work
pRB143	pRB142 with mutated CRP1	This work
pRB144	pRB142 with mutated CRP2	This work
pRB145	pRB142 with mutated CRP1 and CRP2	This work
pRB146	pRB142 with improved CRP2	This work

etry sample cell (cell volume 1.4 ml) was loaded with 84 μM His$_6$-CRP^{Mt}. After a suitable period of thermal equilibration (25 °C), 18 injections of 15 μl of 0.87 mM cAMP were introduced into the protein solution every 6 min with continual stirring and an initial delay of 2 min. A small preinjection of 3 μl was also made to expel any air bubbles that may have accumulated during equilibration. In a separate control experiment, aliquots of the cAMP solution were titrated into the dialysis buffer to determine whether the ligand exhibited heat of dilution. Data analysis and fitting were done using Origin 7.0 (MicroCal LLC), and corrected binding isotherms were best fit using a single set of identical binding sites model as described by Wiseman *et al.* (37).

Transfer of Plasmids, Preparation of Cell-free Extracts, and Assay for β-Galactosidase in M. tuberculosis—These were carried out as described previously (16). β-Galactosidase assays on log phase cultures ($A_{600\ nm} \sim 0.5$) were done according to Miller (38). Three independent cultures were analyzed for each strain.

5′-Rapid Amplification of cDNA Ends—5′-Rapid amplification of cDNA ends was performed using the 5′-rapid amplification of cDNA ends system from Invitrogen according to the manufacturer's instructions. DNA-free RNA (5 μg) from *M. tuberculosis* H37Rv was reverse-transcribed with GSP1 (5′-TACGGGCTTTCGTGCG-3′) using Superscript II reverse transcriptase. The cDNA was purified on a SNAP column and tailed with dCTP using terminal deoxynucleotidyltransferase. The tailed cDNA was amplified using Platinum® Taq with primers GSP2 (5′-CGCCGCTCGTCTTCGCTCAT-3′) and AAP (5′-GGCCACGCGTCGACTAGTACGGGIIGGGIIG-GGIIG-3′). The product was visualized on a 1.5% agarose gel, and a band of ~300 bp was excised and sequenced.

Construction of Reporter Gene Plasmids Using the Upstream Region of whiB1—The region of the DNA sequence upstream of *whiB1* was generated by PCR from *M. tuberculosis* genomic DNA using the primer pairs Myc896 (5′-GCTCTAGAGCAA-GAAAGCGGATCTG-3′) and Myc487 (5′-GCAAGCTTGC-CTTGTGGCGCCAATC-3′) (bp 3,595,415–3,595,731). This fragment was ligated into the XbaI and HindIII sites of the polylinker in the *lacZ* transcriptional reporter plasmid pEJ414 (34) to make pRB142 (P*whiB1*). This construct was verified by DNA sequencing.

Mutagenesis of CRP-binding Site in Plasmid pRB142—This was performed using the Stratagene QuikChange mutagenesis kit. To mutagenize CRP1 (AGTGAGATAGCCCACG to AGT-tAGATAGCCaACG), the primers used were Myc898 (5′-AAC-GAGATCGCCAGAGTTAGATAGCCAACGCGCTTACGT-

AACAC-3′) and Myc899 (5′-GTGTTACGTAAGCGCGTTGGCTATCTAACTCTGGCGATCTCGTT-3′) to generate pRB143. To mutagenize CRP2 (CGTAACACTATTGACA to CcaAACACTATTGACA), the primers used were Myc900 (5′-TAGCCCACGCGCTTACCAAACACTATTGACATCTGTTGAGCCTG-3′) and Myc901 (5′-CAGGCTCAACAGATGTCAATAGTGTTTGGTAAGCGCGTGGGCTA-3′) to generate pRB144. To mutagenize both CRP1 and CRP2, the primers used were Myc963 (5′-CGCCAGAGTTAGATAGCCAACGCGCTTACCAAACACTATTGACATCTGTTG-3′) and Myc964 (5′-CAACAGATGTCAATAGTGTTTGGTAAGCGCGTTGGCTATCTAACTCTGGCG-3′) to generate pRB145. To improve CRP2 (CGTAACACTATTGACA to CGTgACACTATTGACA), the primers used were 5′-TAGCCCACGCGCTTACGTGACACTATTGACATCTGTTGAGCCTG-3′ and 5′-CAGGCTCAACAGATGCACATAGTGTTTGGTAAGCGCGTGGGCTA-3′. Mutagenized constructs were verified by DNA sequencing.

β-Galactosidase Assays in E. coli—Assays were carried out on log phase cultures ($A_{600\ nm} \sim 0.5$) according to Miller (38). Five independent cultures were analyzed for each strain.

Electrophoretic Mobility Shift Assays—The region upstream of the *whiB1* gene was excised from plasmid pGS2060 using restriction enzymes XbaI and HindIII. The resulting fragment was end-labeled using 0.37 MBq of [α-^{32}P]dGTP, dATP, and Klenow enzyme, and unincorporated radionucleotides were removed using a QIAquick PCR clean-up kit (Qiagen). Radiolabeled DNA (~5 ng) was incubated with 0–21 μM His$_6$-CRP^{Mt} (or CRP^{Mt} where indicated) and 0–2 mM cAMP, in the presence of 20 mM HEPES, pH 7.5, 0.2 mM EDTA, 10 mM $(NH_4)_2SO_4$, 1 mM dithiothreitol, 15 mM $MgCl_2$, 15 mM KCl, 0.05 mg ml^{-1} bovine serum albumin, and 0.01 unit of poly(dI-dC), for 30 min at 25 °C. The resulting complexes were then separated on 6% polyacrylamide gels buffered with 0.5× TBE (45 mM Tris borate, 1 mM EDTA).

DNase I Footprinting—Radiolabeled *whiB1* promoter DNA, or *whiB1* promoters with mutated CRP sites (~100 ng), was incubated with 2.5–50 μM His$_6$-CRP^{Mt} in the presence of 50 mM Tris, pH 7.5, 100 mM NaCl, 10 mM $MgCl_2$, and 2 mM cAMP for 30 min at 25 °C. Footprinting reactions containing RNAP were done in the presence of 40 mM Tris, pH 8.0, 75 mM KCl, 10 mM $MgCl_2$, 0.1 mM EDTA, 1 mM dithiothreitol, and 250 μg ml^{-1} bovine serum albumin. The complexes were then digested with 1 unit of DNase I for 15–60 s at 25 °C. Reactions were stopped by the addition of 200 μl of 0.3 M sodium acetate, pH 5.2, containing 20 mM EDTA, followed by phenol/chloroform extraction. The DNA was ethanol-precipitated and resuspended in loading buffer (80% v/v formamide, 0.1% w/v SDS, 10% v/v glycerol, 8 mM EDTA, 0.1% w/v bromphenol blue, 0.1% w/v xylene cyanol) for electrophoretic fractionation on 6% polyacrylamide-urea gels and autoradiographic analysis. Maxam and Gilbert G tracks of the DNA fragments were used to provide a calibration (39).

In Vitro Transcription Reactions and Permanganate Footprinting—M. smegmatis RNAP was isolated by a method adapted from Beaucher *et al.* (40). A 6-g wet cell pellet of *M. smegmatis* mc^2 155 was disrupted by passage through a French pressure cell. The lysate was then centrifuged and subjected to ammonium sulfate precipitation. The resulting cytoplasmic extract was dialyzed against RNAP buffer (50 mM Tris-Cl, pH 8.0, 10 μM $ZnSO_4$, 1 mM EDTA, 10 mM $MgCl_2$, and 20% glycerol) containing 10 mM KCl, before loading onto a 5-ml HiTrap heparin column (GE Healthcare). Elution was achieved by applying a linear gradient of 0.01–1 M KCl in RNAP buffer, and the fractions containing RNAP, as determined by SDS-PAGE, were pooled. Dialysis and purification were repeated twice, using a 1-ml HiTrap SP HP cation exchange column followed by a 1-ml HiTrap Q HP anion exchange column (GE Healthcare). Fractions containing enriched holo-RNAP, as determined by SDS-PAGE, were desalted into RNAP buffer containing 10 mM KCl and concentrated 10-fold using a Vivaspin concentrator (molecular mass cutoff of 5 kDa; Sartorius). The resulting RNAP was then tested in *in vitro* transcription assays (not shown) and stored in 25% glycerol at −80 °C.

For *in vitro* transcription reactions, 0.1–1-kb markers were prepared using Perfect RNA Marker template mix (Novagen). A 20-μl reaction containing 0.75 μg of RNA template mix, 80 mM HEPES, pH 7.5, 12 mM $MgCl_2$, 10 mM NaCl, 10 mM dithiothreitol, 2 mM ATP, 2 mM GTP, 2 mM CTP, 0.1 mM UTP, 5 μCi of [α-^{32}P]UTP (800 Ci mmol^{-1}, PerkinElmer Life Sciences), 20 units of RiboLock RNase inhibitor (Fermentas), and 50 units of T7 RNAP (Novagen), was incubated for 1 h at 37 °C, before storing at −20 °C. Markers from ~2 ng of template were used for gel calibration.

The 285-bp region upstream of the *whiB1* gene and the corresponding regions with the altered CRP^{Mt}-binding sites were excised from plasmids pGS2060, pGS2061, p2225, and p2227 using restriction enzymes XbaI and HindIII. These DNA fragments (0.2 pmol) were incubated for 15 min at 37 °C in a 21-μl reaction volume containing 40 mM Tris-Cl, pH 8.0, 10 mM $MgCl_2$, 1 mM dithiothreitol, 75 mM KCl, 0.1 mM EDTA, 5% glycerol, 250 μg ml^{-1} bovine serum albumin, 0–2 mM cAMP, 2 pmol of *M. smegmatis* RNAP, and 0–20 μM CRP^{Mt}. Transcription was initiated by the addition of 4 μl of a solution containing UTP at 50 μM; ATP, CTP and GTP at 1 mM; and 2.5 μCi of [α-^{32}P]UTP (800 Ci mmol^{-1}, PerkinElmer Life Sciences), followed by incubation for 15 min at 37 °C. Reactions were terminated by the addition of 25 μl of Stop/Loading dye solution (95% formamide, 20 mM EDTA, pH 8, 0.05% bromphenol blue, 0.05% xylene cyanol) containing 0.1–1-kb markers from ~9.5 ng of template as a loading control. Samples (10 μl) of each reaction were loaded onto a 6% acrylamide, 1× TBE, 8 M urea gel and analyzed by autoradiography. Autoradiographs were quantified by ImageMaster software (GE Healthcare).

For permanganate footprinting, the *whiB1* promoter fragment was prepared as for electrophoretic mobility shift assay, except that the opposite strand was end-labeled with [α-^{32}P]dCTP. The resulting radiolabeled DNA (~20 ng) was incubated at 20 °C for 5 min in a reaction containing 40 mM Tris-Cl, pH 8.0, 10 mM $MgCl_2$, 75 mM KCl, 0.1 mM EDTA, 5% glycerol, 250 μg ml^{-1} bovine serum albumin, 0.1 mM GTP, 0.1 mM UTP, 0–2 mM cAMP, and 0–20 μM His-tagged CRP^{Mt}. *M. smegmatis* RNAP (2 pmol) was added and incubation continued at 37 °C for 15 min. $KMnO_4$ (1 mM) was added for 10 min at 37 °C, and the reactions were stopped by the addition of 200 μl of 0.3 M sodium acetate, pH 5.2, containing 20 mM EDTA, fol-

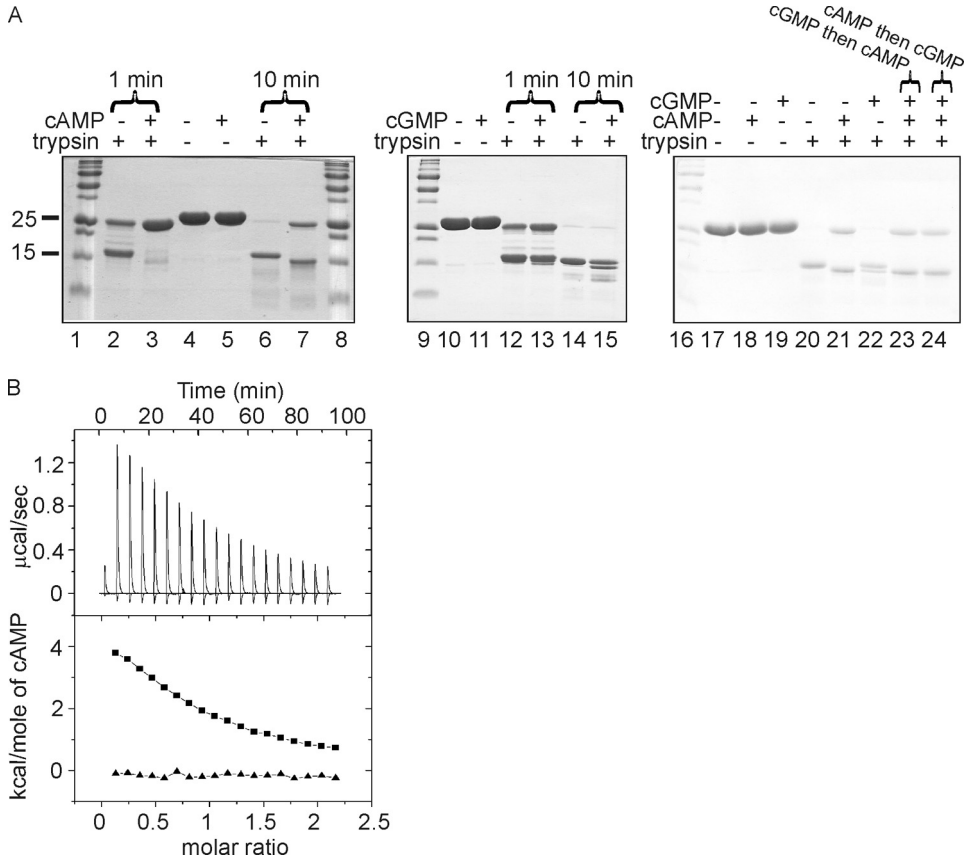

FIGURE 1. **Characterization of cAMP binding by CRP^{Mt}.** *A*, digestion of CRP^{Mt} (15 μg) by trypsin (1 μg) in the presence and absence of cAMP or cGMP (2 mM). The composition of the reaction mixtures is indicated *above* each lane of typical Coomassie Blue-stained SDS-polyacrylamide gels. For *lanes 2, 3, 12,* and *13,* the reactions were incubated at 37 °C for 1 min. For all other lanes, the reactions were incubated at 37 °C for 10 min. *Lanes 1, 8, 9,* and *16* are molecular mass markers; the sizes (kDa) of the relevant markers are shown on the *left* (the full set is 250, 150, 100, 75, 50, 37, 25, 20, 15, and 10 kDa, from *top* to *bottom*). CRP^{Mt} migrates just above the 25-kDa marker. *Lane 23* shows a reaction in which CRP^{Mt} was preincubated for 10 min with cGMP before adding cAMP and trypsin, indicated by *cGMP then cAMP*. *Lane 24* shows a reaction in which CRP^{Mt} was preincubated for 10 min with cAMP before adding cGMP and trypsin, indicated by *cAMP then cGMP*. *B*, analysis of cAMP binding by isothermal calorimetry. The *upper panel* shows the raw binding heats. Integrations of these peaks with respect to time and correction to a per mol basis yield the binding isotherm shown in the *lower panel* (*squares*). Also shown in the lower panel (*triangles*) are the heats of ligand dilution.

lowed by phenol/chloroform extraction and ethanol precipitation. The DNA was then incubated with 10% piperidine at 90 °C for 10 min before being vacuum-dried and resuspended in loading buffer (80% formamide, 0.1% SDS, 10% glycerol, 8 mM EDTA, 0.1% bromphenol blue, 0.1% xylene cyanol) for electrophoretic fractionation on 6% polyacrylamide-urea gels and autoradiographic analysis. A Maxam and Gilbert G track of the DNA fragment was used to provide a calibration (39).

RESULTS

Cyclic AMP Binding at Two Independent Sites Enhances CRP^{Mt}-DNA Interactions—Whereas *E. coli* CRP is very responsive to cAMP, exhibiting nonspecific low affinity DNA binding in the absence of cAMP (27), previous reports of the effects of cAMP on the properties of CRP^{Mt} have been equivocal. Rickman *et al.* (16) and Bai *et al.* (15) found significant binding of CRP^{Mt} to target DNA in the absence of cAMP and only marginal enhancement upon addition of up to 0.1 mM cAMP. In contrast, Agarwal *et al.* (17) failed to detect DNA binding in the absence of cAMP, but binding was observed in the presence of 1 mM cAMP. Others have shown that incubation with cAMP alters intrinsic tryptophan fluorescence (41) and the polypeptide profiles obtained when CRP^{Mt} is digested with trypsin (15), implying that cAMP causes conformational changes in CRP^{Mt}. To investigate further, we have isolated recombinant His$_6$-tagged CRP^{Mt} by overproduction in a *cyaA* mutant of *E. coli*, which is unable to synthesize cAMP. This cAMP-free CRP^{Mt} protein was then used to determine the polypeptide profiles obtained after digestion of CRP^{Mt} with trypsin in the absence and presence of cAMP (Fig. 1*A*, *lanes 2–7*). In contrast to *E. coli* CRP, which is relatively resistant to trypsin cleavage in the absence of cAMP (42), CRP^{Mt} was readily digested by trypsin, yielding a major polypeptide of molecular mass ~16 kDa, as estimated by SDS-PAGE (Fig. 1*A*). In the presence of cAMP, the protein was more resistant to proteolysis, and a major polypeptide of molecular mass ~15 kDa was obtained. In the presence of cGMP, the sensitivity of CRP^{Mt} to trypsin was similar to that observed in the absence of cAMP, although a different digestion pattern, which included both major polypeptides (~16 and ~15 kDa) observed in the absence and presence of cAMP, was obtained suggesting that cGMP is bound by CRP^{Mt} with concomitant changes in conformation that are different from those invoked by cAMP (Fig. 1*A*, *lanes 10–15*). Significantly, addition of cAMP after preincubation with cGMP for 10 min, or vice versa, resulted in a limited proteolysis pattern identical to that obtained with cAMP alone indicating that cAMP is the preferred ligand (Fig. 1*A*, *lanes 20–24*). To ensure that the presence of the His$_6$ tag was not influencing the interaction of CRP^{Mt} with cAMP, the His$_6$ tag was removed by thrombin cleavage, and the partial proteolysis experiments were repeated. This showed that untagged CRP^{Mt} exhibited the same behavior as the tagged protein in the absence (supplemental Fig. S1, *lanes 3* and *6*) and presence (supplemental Fig. S1, *lanes 4* and *7*) of cAMP suggesting that the His$_6$ tag was not affecting the gross conformational changes induced by cAMP binding. Therefore, the His$_6$-tagged form of CRP^{Mt} was considered suitable for further ligand binding studies.

Isothermal calorimetry was used to determine the stoichiometry and affinity of cAMP binding to His$_6$-CRP^{Mt}. A typical

titration is shown in Fig. 1*B*. The data yield good nonlinear least squares fitting to a single set of identical binding sites model and are consistent with each protomer of the CRP^{Mt} dimer binding one cAMP molecule with relatively weak (K_b of ~1.7×10^4 M^{-1}) affinity. Furthermore, the binding of cAMP is an endothermic reaction (ΔG_b −23.7 kJ mol^{-1}) with a positive binding enthalpy (ΔH_b ~ 30.7 kJ mol^{-1}). Therefore, the entropy change $T\Delta S_b$ is ~54.4 kJ mol^{-1} K^{-1}, and hence cAMP binding is entropically driven. Chemical cross-linking showed that CRP^{Mt} is a dimer (not shown), and thus the data indicate that unlike the *E. coli* CRP dimer, the two cAMP-binding sites in the CRP^{Mt} dimer are independent.

The effect of cAMP binding on the ability of CRP^{Mt} to bind DNA *in vivo* was tested in the heterologous host *E. coli* because *M. tuberculosis* has 17 predicted adenylyl cyclase proteins, and *E. coli* has only one, CyaA; and thus it is possible to simply create a cAMP-free background for these experiments. The parent *E. coli* strain was a *crp lac* double mutant into which a *cyaA* mutation was introduced. The readout (β-galactosidase activity) from the simple CRP-repressed promoter CCgalΔ4, which contains a consensus CRP site that is recognized by CRP^{Mt} located such that occupation of this site occludes the promoter (18, 34), was used as a measure of the DNA binding activity of CRP^{Mt} as shown previously by Spreadbury *et al.* (18). In the CyaA$^+$ and CyaA$^-$ strains containing the vector (ptac85), transcription from the reporter was similar (761 ± 24 and 722 ± 25 Miller units, respectively, $n = 5$). However, in the presence of the CRP^{Mt} expression plasmid (pGS1645), reporter transcription was ~60% lower (323 ± 86 Miller units, $n = 5$) in the Cya$^+$ strain compared with that observed in the absence of CRP^{Mt}, consistent with the observations of Spreadbury *et al.* (18). However, in the *cyaA* mutant, which is unable to synthesize cAMP, the readout from the reporter in the presence of CRP^{Mt} increased by ~2-fold (613 ± 20 Miller units, $n = 5$) compared with the Cya$^+$ strain to reach ~80% of the activity observed in the absence of CRP^{Mt}. These data are consistent with cAMP enhancing DNA binding of CRP^{Mt} *in vivo*.

To investigate the effect of cAMP on CRP^{Mt} DNA binding *in vitro*, preliminary electrophoretic mobility shift assays were used to show that CRP^{Mt} formed at least two complexes at the *whiB1* promoter in the absence and presence of cAMP but that DNA binding was enhanced in the presence of cAMP (supplemental Fig. S2*A*). Furthermore, in cAMP titration experiments, CRP^{Mt} binding to the *whiB1* promoter was enhanced when the cAMP concentration exceeded 0.05 mM (not shown), consistent with the isothermal calorimetry experiments. Moreover, the presence of the His_6 tag did not significantly affect DNA binding by CRP^{Mt} in the absence (not shown) and presence of cAMP (supplemental Fig. S2*B*). Thus, the His_6-tagged form was used in further DNA binding studies.

In summary, the work described above shows the following: (i) that CRP^{Mt} binds two cAMP molecules per dimer (one per subunit); (ii) that the cAMP-binding sites act independently; and (iii) that cAMP binding induces conformational changes in the CRP^{Mt} dimer that enhance specific DNA binding *in vitro* and *in vivo*.

whiB1 Promoter Contains Two CRP^{Mt}-binding Sites—The *whiB1* gene encodes a Wbl (WhiB-like) protein. These proteins

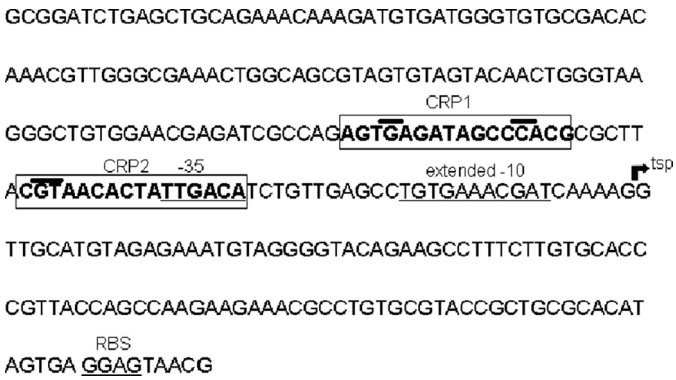

FIGURE 2. **Nucleotide sequence of the *whiB1* promoter region (P*whiB1*).** Diagram of the nucleotide sequence of P*whiB1* showing the transcript start (*tsp*) and its associated extended −10 region and −35 region (*underlined*), two CRP^{Mt}-binding sites (*boxed*), and the ribosome-binding site (*RBS*). The locations of the nucleotides within the CRP^{Mt}-binding sites that were replaced to impair the sites as indicated in the text are *overlined*.

have iron-sulfur clusters and are found only in actinomycetes (26) where they are thought to function as transcription factors and/or as protein-disulfide reductases. The *whiB1* transcript was less abundant in a CRP^{Mt} mutant (16), implying that CRP^{Mt} activates *whiB1* expression, which was confirmed using a *whiB1-lacZ* fusion (17). 5′-Rapid amplification of cDNA ends was used to confirm that the *whiB1* transcript start was located at 109 or 110 bp upstream of the translational start as reported by Agarwal *et al.* (17) (data not shown). The electrophoretic mobility shift assays (supplemental Fig. S2*A*) suggested the presence of more than one CRP^{Mt}-binding site in the *whiB1* promoter. Inspection of the *whiB1* promoter region indicated the presence of two potential CRP^{Mt}-binding sites upstream of the transcript start (Fig. 2). The first site (CRP1) located at −58.5 relative to the transcript start matches the proposed CRP^{Mt} consensus (NGTGNNANNNNNCACA) of Rickman *et al.* (16) in seven of the eight defined bases (Fig. 2). The second potential site (CRP2) is a poorer match to the consensus (six of the eight defined bases are matched) and is located at −37.5 relative to the transcript start. The CRP1 site has previously been implicated in CRP^{Mt}-dependent activation of *whiB1* expression (17).

DNase I footprinting showed that both CRP1 and CRP2 sites in the *whiB1* promoter were recognized by CRP^{Mt} and that binding to both sites was enhanced in the presence of cAMP (Fig. 3*A*). Titration of the *whiB1* promoter with increasing concentrations of CRP^{Mt} showed that the CRP1 site (−70 to −51) was occupied before the CRP2 site (−50 to −29) (Fig. 3*A*). Furthermore, mutation of CRP1 (indicated by lowercase letters, AGTGAGATAGCCCACG to AGTtAGATAGCCaACG) or CRP2 (CGTAACACTATTGACA to CcaAACACTATTGACA) inhibited binding of CRP^{Mt} to these sites (Fig. 3*B*). Inactivation of CRP1 also impaired, but did not abolish, binding to CRP2 (Fig. 3*B*, compare *lane 5* with *6*). Thus, it was concluded: (i) the *whiB1* promoter possesses tandem CRP^{Mt} sites, (ii) binding to these sites is enhanced in the presence of cAMP; and (iii) occupation of CRP2 is improved by occupation of CRP1.

Both CRP^{Mt}-binding Sites in the whiB1 Promoter Are Functional—The DNase I footprinting studies indicated that there are two *CRP^{Mt}* sites in the *whiB1* promoter. The function-

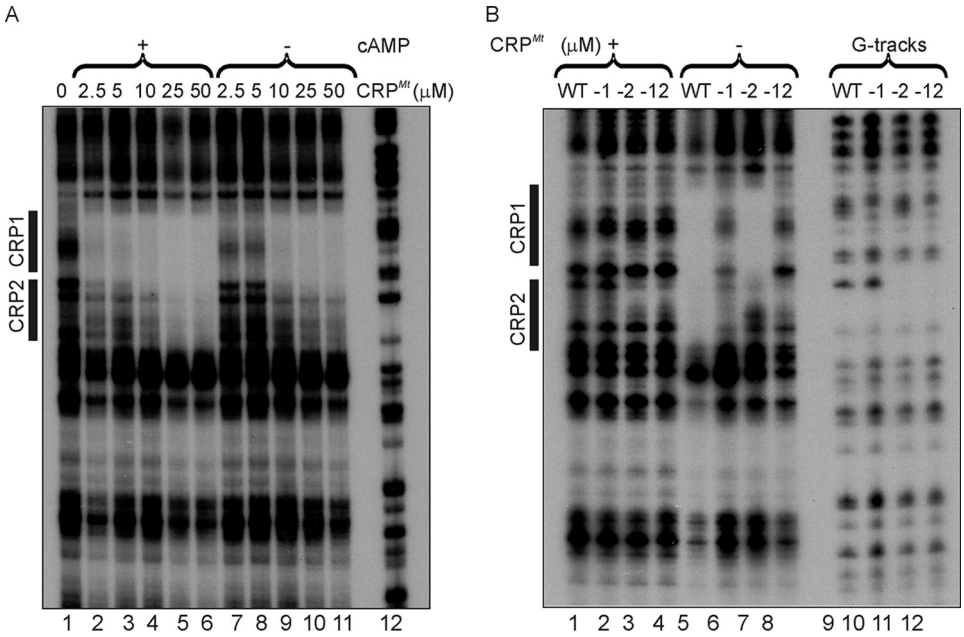

FIGURE 3. **Identification of two CRP^{Mt}-binding sites within P*whiB1*.** *A*, *whiB1* promoter (P*whiB1*) has two CRP^{Mt}-binding sites. *Lanes 2–6* show reactions in the presence of 2 mM cAMP; *lanes 7–11* show reactions in the absence of cAMP. *Lane 1* shows no CRP^{Mt}; *lanes 2* and *7* show 2.5 μM CRP^{Mt}; *lanes 3* and *8* show 5 μM CRP^{Mt}; *lanes 4* and *9* show 10 μM CRP^{Mt}; *lanes 5* and *10* show 25 μM CRP^{Mt}; *lanes 6* and *11* show 50 μM CRP^{Mt}; *lane 12* shows Maxam and Gilbert G track. *WT*, wild type. *B*, mutation of P*whiB1* CRP1 impairs binding of CRP^{Mt} to CRP2. All reactions contained cAMP (2 mM). *Lanes 1–4* show reactions of the indicated promoter variants in the absence of CRP^{Mt} as follows: *−1*, CRP1 site impaired (AGTGAGATAGCCCACG to AGTtAGATAGCCaACG); *−2*, CRP2 site impaired (CGTAACACTATTGACA to CcaAACACTATTGACA), and *−12*, both sites impaired. *Lanes 5–8*, DNase I footprints in the presence of 50 μM CRP^{Mt}. *Lanes 9–12*, Maxam and Gilbert G tracks. The locations of the CRP1 and CRP2 sites (see Fig. 2) are indicated by *boxes*. The footprints shown are typical of at least three experiments.

ality of the sites was tested by *in vitro* transcription experiments. Transcription from the *whiB1* promoter in the presence of *M. smegmatis* RNAP was low (Fig. 4*A*, *lane 3*). At low concentrations of CRP^{Mt}, *whiB1* transcription was enhanced, but at higher concentrations CRP^{Mt} inhibited transcription (Fig. 4*A*, *lanes 4–8*). This same pattern of regulation was observed with the untagged form of CRP^{Mt} (supplemental Fig. S3, compare *lanes 3–6* and *lanes 7–10*), indicating that the presence of the His_6 tag does not alter the transcriptional behavior of CRP^{Mt}. A similar transcription profile was observed in the presence of cAMP (Fig. 4*A*, *lanes 9–16*) except for the following: (i) there was a reproducible decrease in basal transcription (Fig. 4*A*, compare *lanes 3* and *11*), and (ii) the response curve was shifted to the left, with maximum *whiB1* expression occurring in the presence of 1.3 μM CRP^{Mt} in the presence of cAMP compared with 2.5 μM CRP^{Mt} in the absence of cAMP (Fig. 4*B*). This result is consistent with cAMP enhancing CRP^{Mt} binding to both CRP1 and CRP2 sites in the *whiB1* promoter. In conjunction with the footprinting experiments described above, these data were interpreted to mean that binding to the high affinity CRP1 site activates *whiB1* transcription, whereas occupation of both CRP1 and CRP2 sites inhibits *whiB1* transcription. This conclusion was supported by *in vitro* transcription reactions with *whiB1* promoters carrying mutations in CRP1 and/or CRP2 (Fig. 4*C*). At a low CRP^{Mt} concentration (2.5 μM) in the absence of cAMP, the footprinting evidence indicates that CRP1 will be occupied at the wild-type promoter. Under these conditions, mutation of the CRP1 site decreased transcription of *whiB1* (Fig. 4, *C* and *D*, *lanes 1* and *2*). Under the same conditions, mutation of CRP2 slightly enhanced *whiB1* transcription (Fig. 4, *C* and *D*, *lanes 1* and *3*). A similar pattern was observed in the presence of cAMP (Fig. 4, *C* and *D*, *lanes 5–7*). At a higher CRP^{Mt} concentration (20 μM), the footprints indicate that both CRP1 and CRP2 will be occupied. Under these conditions, impairment of CRP1 had little effect on transcription compared with the wild-type promoter, *i.e.* transcription remained low (Fig. 4, *C* and *D*, *lanes 9* and *10* and *lanes 13* and *14*). However, impairment of CRP2 enhanced transcription of *whiB1* compared with the wild-type promoter under these conditions (Fig. 4, *C* and *D*, *lanes 9* and *11*, and *lanes 13* and *15*). Hence, these observations suggest that occupation of CRP2 is sufficient to repress basal transcription from P*whiB1*. In the presence of cAMP, mutation of both CRP^{Mt} sites resulted in transcription similar to that of the unaltered promoter in the absence of CRP^{Mt} (Fig. 4, *C* and *D*, *lanes 8* and *16*). In the absence of cAMP, transcription from the *whiB1* promoter with both CRP1 and CRP2 impaired was lower than from the unaltered promoter in the absence of CRP^{Mt}, suggesting that in the absence of cAMP there is still some unproductive interaction between CRP^{Mt} and the altered *whiB1* promoter despite the impairment of both CRP-binding sites (Fig. 4, *C* and *D*, *lanes 4* and *12*). Note that transcription in the absence of CRP^{Mt} for all the altered promoters was the same as that for the unaltered *whiB1* promoter, indicating that the changes to the sequences of the CRP sites had not affected the basal level of transcription (data not shown).

The *in vitro* transcription experiments showed that CRP^{Mt} acts as both an activator (at low concentrations) and repressor (at high concentrations) of *whiB1* expression. Permanganate footprinting to detect open complex formation showed the presence of quantitatively similar distortions of DNA at nucleotide T −8 in the *whiB1* promoter mediated by RNAP in the presence or absence of 2.5 μM CRP^{Mt} (Fig. 5*A*, *lanes 3, 4, 8,* and *9*). This evidence suggests that CRP^{Mt}-mediated activation of *whiB1* expression probably occurs after open complex formation, because in the absence of CRP^{Mt} transcription from the *whiB1* promoter is low (Fig. 4*A*, compare *lanes 3* and *4*). In the presence of 20 μM CRP^{Mt}, the open complex was not detected (Fig. 5*A*, *lanes 5* and *10*) indicating that higher concentrations of CRP^{Mt} inhibit *whiB1* expression at a point before open complex formation, probably by inhibiting RNAP binding.

DNase I footprinting of the *whiB1* promoter in the presence of *M. smegmatis* RNAP and activating concentrations of CRP^{Mt} (2.5 μM) showed that RNAP could bind at the promoter when

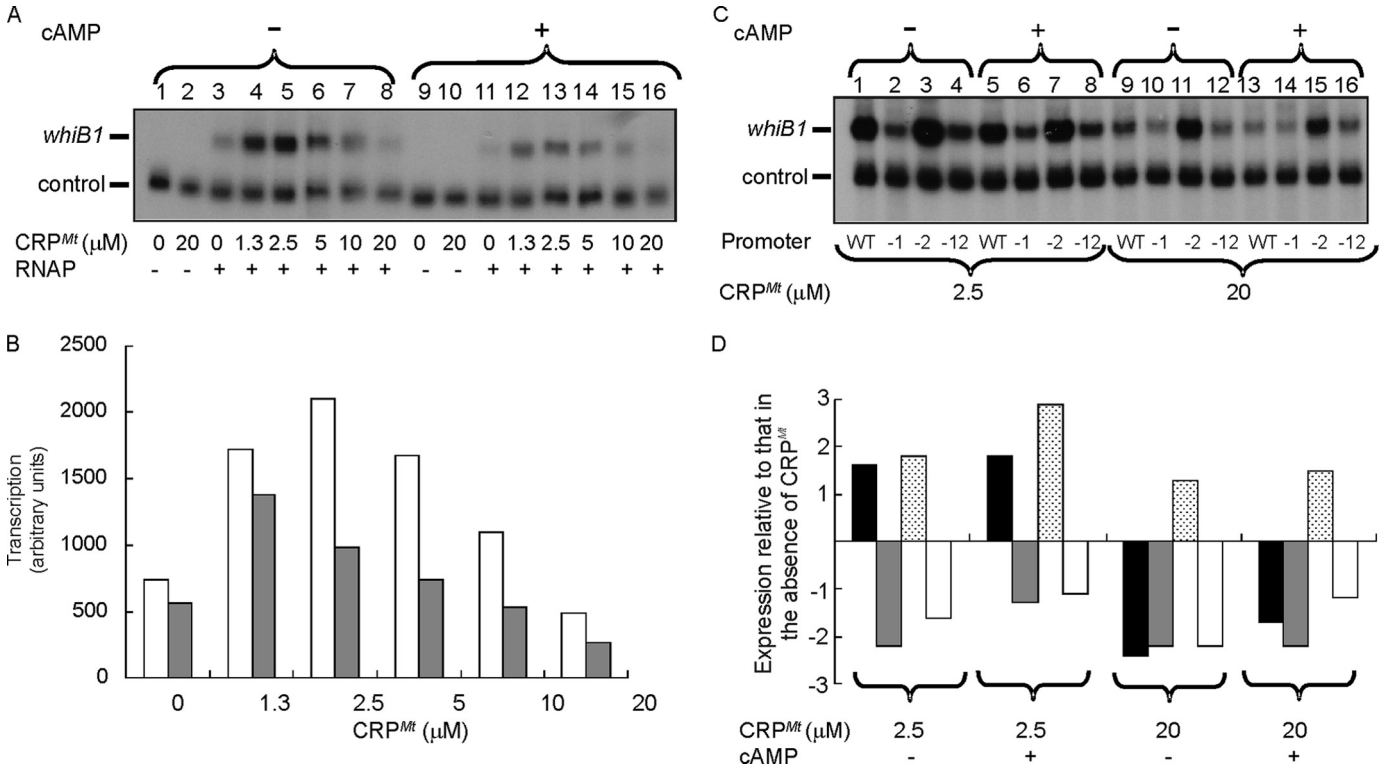

FIGURE 4. ***In vitro* transcription from P*whiB1* is activated by CRP^{Mt} occupation of CRP1 and inhibited by CRP^{Mt} occupation of CRP2.** Reactions were carried out as described under "Experimental Procedures" with the amounts of CRP^{Mt} used shown *below* each lane. *A*, typical autoradiograph showing the effects of increasing concentrations of CRP^{Mt} on *whiB1* transcription *in vitro*. *B*, using the control as the standard, the relative amount of *whiB1* transcript in each of the reactions shown in *A* was quantified and plotted as a *histogram*. *Open bars,* no cAMP; *filled bars*, 2 mM cAMP. *C*, *autoradiograph* showing the effects of mutation of the *whiB1* CRP^{Mt}-binding sites on transcription. The *whiB1* promoter variants are as described in Fig. 3*B*. The control and the *whiB1* transcript are indicated. WT, wild type. *D*, using the amount of transcript formed in the absence of CRP^{Mt} as the base line, the amount of transcript formed under the indicated conditions was quantified and plotted as a *histogram* (*black bars,* wild-type promoter; *gray bars*, CRP1 impaired; *stippled bars*, CRP2 impaired; *open bars*, CRP1 and CRP2 impaired). The *in vitro* transcriptions shown are typical of at least three experiments. The amount of transcription relative to that observed in the absence of CRP^{Mt} was calculated by dividing the mean of the test condition by that measured in the absence of CRP^{Mt} and expressing this value as a fold difference.

the CRP1 site was occupied and that this was accompanied by the appearance of an RNAP-dependent hypersensitive site at position −34, which is within the CRP2 site (Fig. 5*B*). The presence of the hypersensitive site is attributed to docking of the C-terminal domain of the RNAP α-subunit downstream of CRP^{Mt} bound at CRP1.

To determine whether the effects of CRP^{Mt} on *whiB1* transcription observed *in vitro* were also apparent *in vivo*, a promoter fusion containing DNA from −187 to 129 relative to the transcript start was fused upstream of a *lac* reporter gene, and transcription was estimated in *M. tuberculosis* wild-type H37Rv and an isogenic *Rv3676* (*crp*) mutant (Fig. 6). Under exponential growth conditions, expression of *whiB1* was decreased by ~3-fold in the CRP^{Mt} mutant (ΔRv3676), consistent with CRP^{Mt}-dependent activation. An ~5-fold reduction in expression was observed when the CRP1 site was disabled, reflecting the absence of activation from CRP1 but retention of repression from CRP2. Accordingly, mutation of CRP2, without disrupting the −35 element (underlined) of the *whiB1* promoter (CGTAACACTATTGACA to CcaAACACTATTGACA), resulted in a small but reproducible increase in *whiB1* expression. Similarly, improvement of the CRP2 site (CGTAACACTATTGACA to CGTgACACTATTGACA) caused a reproducible decrease in *whiB1* expression. Disabling both CRP1 and CRP2 lowered β-galactosidase activities by an amount similar to that observed using the unaltered promoter in the *crp* mutant. The *in vivo* data correlated well with the *in vitro* transcription data as shown in Fig. 4, *C* and *D*. Thus, when 2.5 μM CRP^{Mt} was used in the *in vitro* transcription reactions (Fig. 4*D*), the fold changes in transcription upon impairment of CRP-binding sites compared with the unaltered promoter were as follows: −3.5 to −2.4 when CRP1 was impaired; +1.2 to +1.6 when CRP2 was impaired; and −2.6 to −2.0 when both CRP1 and CRP2 were impaired. These values are similar to those obtained for transcription *in vivo* (Fig. 6) as follows: −4.6 when CRP1 was impaired; +1.2 when CRP2 was impaired; and −2.0 when CRP1 and CRP2 were impaired. Hence, the *in vitro* and *in vivo* experiments are consistent with a mechanism in which occupation of CRP1 enhances *whiB1* expression, whereas occupation of both CRP1 and CRP2 or of CRP2 alone represses *whiB1* expression in *M. tuberculosis*.

DISCUSSION

The work described here shows that CRP^{Mt} is a homodimeric protein with one cAMP-binding site per protomer. This conclusion is substantiated by the crystal structure of CRP^{Mt} bound to cAMP that was published during the review of this manuscript (43). For *E. coli* CRP, cAMP binding is cooperative; the first binding event is exothermic and the second is endothermic, and the sensory domain binding sites are satu-

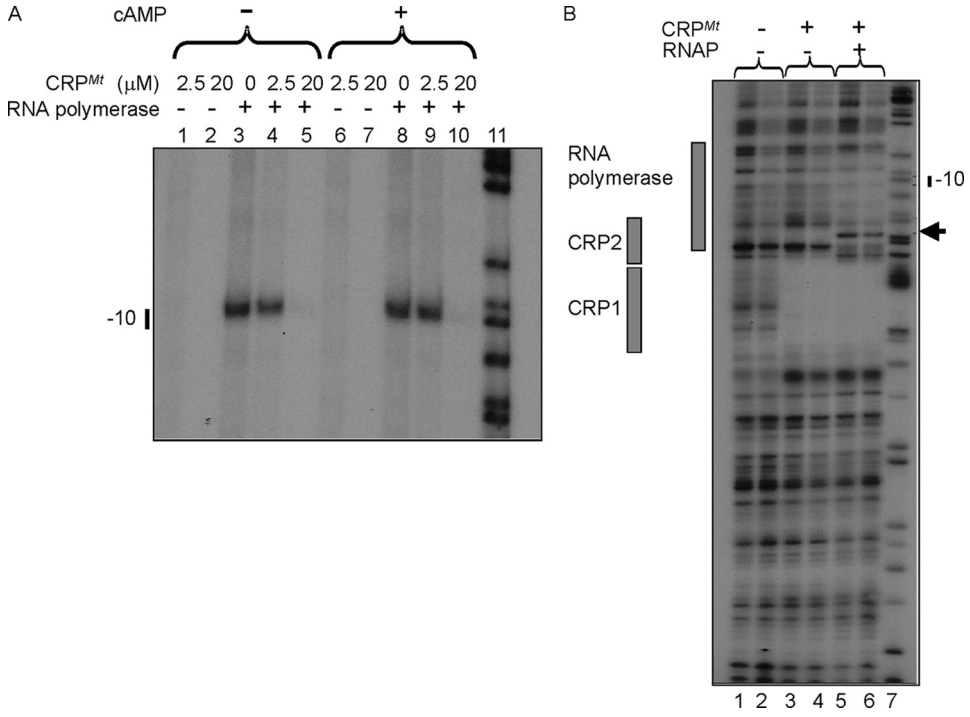

FIGURE 5. ***M. tuberculosis* CRP activates *whiB1* transcription after open complex formation.** *A*, permanganate footprints were obtained with P*whiB1* in the presence and absence of *M. smegmatis* RNAP and CRP^{Mt}. *Lanes 1* and *6* show CRP^{Mt} 2.5 μM only; *lanes 2* and *7* show CRP^{Mt} 20 μM only; *lanes 3* and *8* show RNAP only; *lanes 4* and *9* show RNAP plus CRP^{Mt} 2.5 μM; *lanes 5* and *10* show RNAP plus CRP^{Mt} 20 μM; *lane 11* shows Maxam and Gilbert G track. *Lanes 1–5* show reactions in the absence of cAMP; *lanes 6–10* show reactions in the presence of cAMP (2 mM). The location of the −10 element is indicated. *B*, DNase I footprint of P*whiB1* in the presence of an activating concentration of CRP^{Mt} (2.5 μM) and RNAP. *Lanes 1* and *2* show no protein; *lanes 3* and *4* show CRP^{Mt}; *lanes 5* and *6* show CRP^{Mt} plus RNAP; *lane 7* shows Maxam and Gilbert G track. The locations of the CRP1 (protected) and CRP2 (unprotected) sites are indicated by *filled rectangles*, as is the region of protection afforded by RNAP. The location of the −10 element is also marked. The hypersensitive site within CRP2 that appears in the presence of RNAP is indicated by the *arrow*. The footprints shown are typical of at least three experiments.

rated by micromolar concentrations of cAMP (44). This is not the case for CRP^{Mt} where the cAMP-binding sites are independent. The cAMP binding parameters for CRP^{Mt} are similar to those for cGMP binding to *E. coli* CRP, except that the thermodynamic properties of these interactions are opposite; CRP^{Mt} cAMP binding has a positive enthalpy, whereas *E. coli* CRP cGMP binding is exothermic (44). Recently, cAMP binding by *E. coli* CRP has been shown to reorganize the major helices that form the dimer interface, thereby rotating the DNA binding domains so that they can interact with adjacent major grooves in target DNA (45). The differences in binding of cAMP by the *E. coli* and *M. tuberculosis* CRP proteins suggest that the signal transduction pathways that promote site-specific DNA binding might be different, and this might be reflected in the relatively small enhancement in DNA binding caused by addition of cAMP.

Comparison of the cAMP binding pockets of CRP^{Mt} (44) and *E. coli* CRP (46, 47) reveals that most of the side chains that contact cAMP are either conserved or are conservatively substituted. The significant difference between the two proteins, in the context of the independent cAMP binding of CRP^{Mt} compared with the cooperative cAMP binding of *E. coli* CRP, is the substitution of Ser-128 in *E. coli* CRP by Asn in CRP^{Mt}. Ser-128 makes a cross-subunit contact with cAMP in *E. coli* CRP; *i.e.* Ser-128 of subunit B interacts with cAMP bound at subunit A (46, 47). Fig. 7 shows that the N6 position of cAMP is able to donate two hydrogen bonds, which interact with the acceptor γ oxygen atoms of Thr-127 of one subunit (subunit A) and of Ser-128 in the other subunit (subunit B) in *E. coli* CRP. The latter two atoms are constrained to act as acceptors because they in turn donate hydrogen bonds to the main chain carbonyl acceptors of residues 123 in subunit A and 124 in subunit B, respectively. Residues 123 and 124 are located in the dimerization helices of the two *E. coli* CRP subunits. The N6 of the adenosine moiety of cAMP therefore acts via Thr-127 of subunit A and Ser-128 of subunit B as a bridge between the main chains of the dimerization helices of the two subunits (Fig. 7*A*). A reciprocal interaction occurs when cAMP is bound in the other site of the CRP dimer, and hence the cAMP-binding sites of each protomer are connected. In CRP^{Mt}, the equivalent position to Ser-128 is occupied by Asn-135, and this does not significantly alter the position of cAMP. However, the Asn side chain makes two hydrogen bonds to cAMP; the ND2 of the Asn side chain can donate an H bond to the N7 of cAMP, and the OD1 atom can accept a hydrogen bond from one of the N6 donor hydrogen atoms (Fig. 7*B*). This pattern of interactions removes the possibility of the side chain of Asn-135 donating a hydrogen bond to the main chain carbonyl of residue 131 of subunit B. For this reason, replacement of the Ser by Asn at this position uncouples the cAMP-binding sites in CRP^{Mt}. Consistent with this interpretation, the substitution of Ser-128 by Ala in *E. coli* CRP abolishes cooperative cAMP binding (48).

Although cAMP enhanced binding of recombinant CRP^{Mt} to target DNA, this enhancement was not comparable with that observed with *E. coli* CRP, where DNA-binding affinity is enhanced by several orders of magnitude in the presence of 0.1 mM cAMP, allowing specific DNA binding at nanomolar concentrations (27, 48). For CRP^{Mt}, a much less significant enhancement of DNA binding was observed, and higher concentrations of cAMP compared with *E. coli* CRP were required. This may point to meaningful physiological changes in cAMP concentration in *M. tuberculosis* occurring at higher levels than those in *E. coli*. Indeed, cAMP concentrations in mycobacteria have been reported to be rather high (49), being ~100–200-fold greater than for *E. coli*. The high intracellular concentration of cAMP in *M. tuberculosis* is consistent with the numerous adenylyl cyclases synthesizing cAMP. This and the reported increase in cAMP levels that occurs after infection of

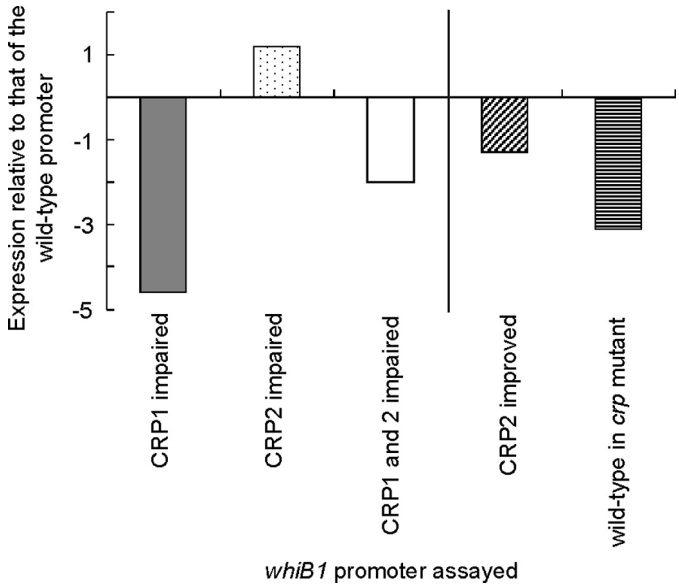

FIGURE 6. **Patterns of *whiB1* expression *in vivo* match those seen *in vitro*.** β-Galactosidase assays were performed on cell extracts from *M. tuberculosis* H37Rv strains containing constructs with P*whiB*1 promoter linked to the *lacZ* reporter gene. These were as follows: the unaltered P*whiB1* (wild-type), P*whiB1* with the CRP1 site impaired (*CRP1 impaired*), P*whiB1* with the CRP2 site impaired (*CRP2 impaired*), and P*whiB1* with both the CRP1 and CRP2 sites impaired (*CRP1 and 2 impaired*). The effects of the mutations made in the CRP sites are shown as expression relative to that of the unaltered wild-type promoter to allow direct comparison with the *in vitro* transcription assays in Fig. 4*D*. Thus, the result for P*whiB1* with an impaired CRP1 site is shown as a *gray bar*; the result for P*whiB1* with an impaired CRP2 site is shown as a *stippled bar*, and the result for P*whiB1* with impaired CRP1 and CRP2 sites is shown as an *open bar*. In addition, on the *right* of the figure, the effect of improving the CRP2 site of P*whiB1* (CRP2 improved; *diagonal stripes*) as well as expression from unaltered P*whiB1* in H37Rv ΔRv3676 (wild-type in *crp* mutant strain; *horizontal stripes*) is shown. The values shown are calculated from the mean β-galactosidase activities from three bacterial cultures. All assays were done in triplicate and varied by <15%. The expression relative to the unaltered *whiB1* promoter in *M. tuberculosis* H37Rv was calculated by dividing the mean of the test condition by that obtained for the wild-type promoter and expressing this value as a fold change.

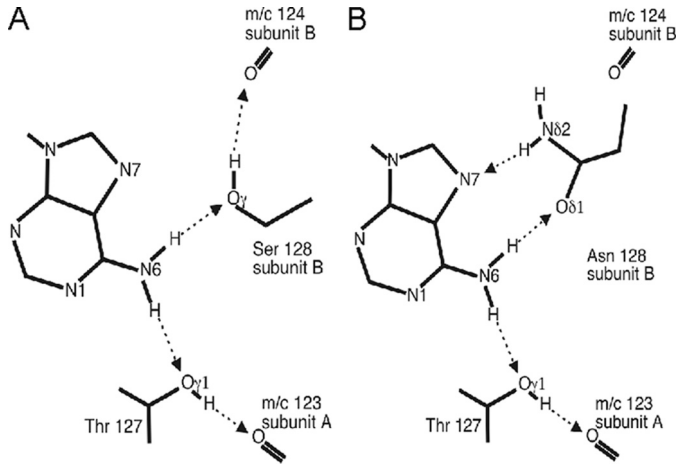

FIGURE 7. **Schematic diagram of hydrogen bonding contacts of the adenine groups of cAMP in the binding pockets of *E. coli* and *M. tuberculosis* CRP proteins.** *A*, observed hydrogen bonds between cAMP and *E. coli* CRP (Protein Data Bank code 2cgp) (45). *B*, predicted hydrogen bonds between cAMP and CRP^{Mt} in which Ser-128 is replaced by Asn. Hydrogen bonds are shown as *dotted arrows* from donor to acceptor. Atoms referred to in the text are labeled.

macrophages by pathogenic mycobacteria (5–7) point to cAMP being an important signaling molecule in infection. The evidence presented here suggests that, perhaps as a consequence of the high intracellular concentrations of cAMP in *M. tuberculosis*, CRP^{Mt} has evolved a different mode of interaction with cAMP compared with the *E. coli* paradigm, involving low affinity binding of cAMP to independent sites. Nevertheless, the response of CRP^{Mt} to cAMP was very significant for expression of *whiB1*.

Several different classes of regulated bacterial promoters have been identified based on the locations of the binding sites for transcription activators. Promoters dependent on transcription factors bound at or close to −61 are known as class I promoters (Fig. 8). At these promoters a specific region, known as activating region 1 (AR1), of the transcription factor interacts with the *C*-terminal domain of the α-subunit (α-CTD) of RNAP to activate transcription. A common alternative architecture is that of the class II promoters, in which the transcription factor binds to a site that overlaps the core −35 element of the promoter. At class II promoters multiple interactions between the transcription factor and RNAP are possible, including an AR1 interaction with α-CTD, an AR2 interaction with the RNAP α-subunit N-terminal domain, and interaction between AR3 and the σ-subunit of RNAP (Fig. 8). Class III promoters have transcription factors bound in tandem making both class I- and class II-type interactions with RNAP (Fig. 8). The experiments described here and elsewhere show that expression of *whiB1* is dependent on CRP^{Mt} and that this requires a CRP^{Mt}-binding site centered 58.5 bp upstream of the transcript start, a class I location (16, 17). However, it is now shown that there is a second, lower affinity, negatively acting CRP-binding site (CRP2 centered at −37.5) located immediately downstream of CRP1 that has significant implications for cAMP-CRP^{Mt}-mediated regulation of *whiB1* expression. The identification of a second class II CRP^{Mt}-binding site (CRP2) that is occupied when cAMP levels increase and inhibits *whiB1* activation by CRP^{Mt} bound at the class I site (CRP1) indicates that *whiB1* expression *in vivo* should be maximal at intermediate cAMP concentrations. Hence, the following model for cAMP-responsive *whiB1* expression provides the simplest explanation for the data described here. The locations of the two CRP^{Mt}-binding sites (−58.5 and −37.5) are such (centers of the sites are separated by 21 bp) that they are located on the same face of the DNA helix. At low concentrations of the CRP^{Mt}-cAMP complex, CRP1 is preferentially occupied (Fig. 3*A*); the α-CTD of RNAP docks downstream of CRP1 (Fig. 5*B*), and transcription of *whiB1* is activated via a class I mechanism (Fig. 8). Activation of class I promoters by *E. coli* CRP occurs solely by recruiting RNAP to the promoter by increasing the binding constant for the formation of the RNAP-promoter closed complex (reviewed in Ref. 10). However, the permanganate footprints suggest that low (nonrepressing; Fig. 4*A*) concentrations of CRP^{Mt} or CRP^{Mt}-cAMP do not significantly enhance open complex formation at the *whiB1* promoter compared with reactions lacking CRP^{Mt} (Fig. 5*A*) indicating that a step after open complex formation is activated. Further experimental work will be needed to identify the mechanism by which this is achieved.

At higher CRP^{Mt} or CRP^{Mt}-cAMP concentrations, both CRP1 (class I position) and CRP2 (class II position) are occupied (Fig. 3*A*). Occupation of both CRP1 and CRP2 sites would

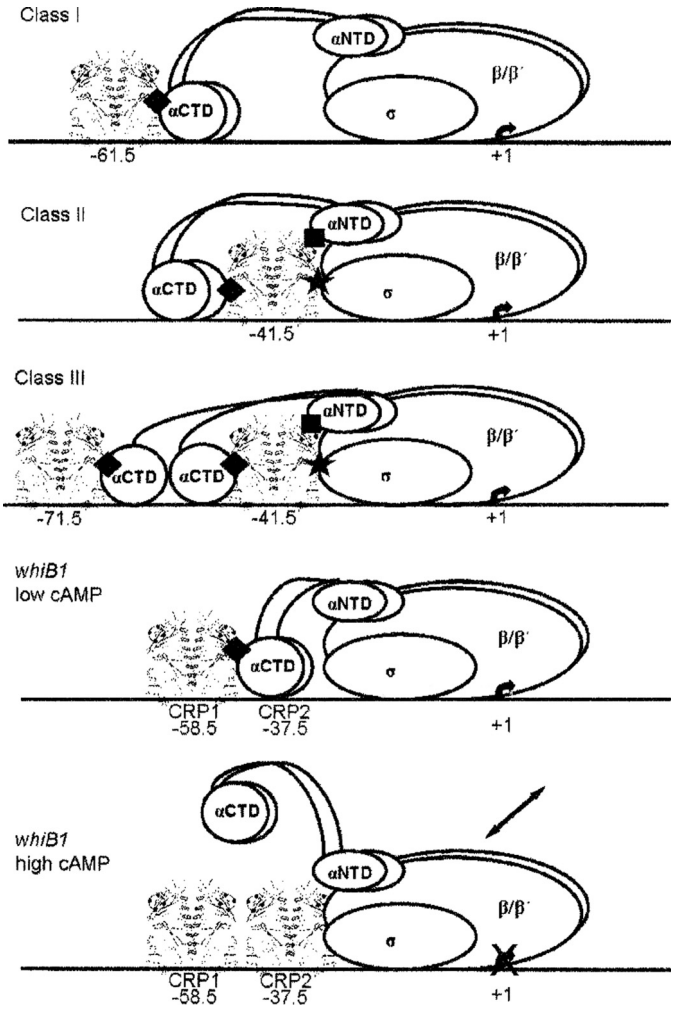

FIGURE 8. **Architecture of CRP-dependent promoters.** The diagram shows the arrangement of nucleoprotein complexes formed at typical class I, class II, and class III CRP-dependent promoters. At class I promoters, the center of the CRP dimer (shown in ribbon form) is positioned at −61.5, −71.5, −81.5, or −91.5 upstream of the transcript start, placing it on the same face of the DNA helix (*horizontal line*) as RNAP (shown as *unfilled ellipses*). This arrangement allows the C-terminal domain of the RNAP α-subunit (α-CTD) to interact directly with activating region 1 (*AR1*) of the downstream subunit of the CRP dimer (◆). At class II promoters, the CRP dimer is centered at or close to −41.5 and is again on the same face of the DNA helix as RNAP. At these promoters multiple interactions between CRP and RNAP are possible, with contacts between AR1 of the upstream subunit of the CRP dimer and α-CTD, and between activating region 2 (AR2) of the downstream subunit of the CRP dimer and the N-terminal domain of the RNAP α-subunit (α-*NTD*; ■), and activating region 3 (*AR3*) of the same CRP subunit and the RNAP σ factor (★). Class III promoters have tandem CRP sites in class I and class II locations allowing AR1, AR2, and AR3 contacts with RNAP. For *E. coli* CRP, these protein-protein interactions recruit RNAP to CRP-dependent promoters (10). For *M. tuberculosis* P*whiB1* at low cAMP-CRP^{Mt} concentrations, CRP1 is occupied and expression is activated, not by RNAP recruitment but by enhancing a step after open complex formation, *i.e.* promoter clearance. At high cAMP-CRP^{Mt} concentrations, CRP1 and CRP2 are occupied. This arrangement has some similarities with the class III architecture, but because the CRP1 and CRP2 sites are immediately adjacent, there is insufficient space to accommodate the α-CTD between the tandem CRP dimers resulting in inhibition of transcription by preventing α-CTD from docking with DNA thereby inhibiting productive interaction of RNAP with P*whiB1* (indicated by the *double-headed arrow*).

leave little space between the two CRP^{Mt} dimers, preventing the formation of a typical class III nucleoprotein complex and thus the RNAP α-CTD is displaced, which is likely to result in either poor or unproductive binding of RNAP to the *whiB1* promoter (Fig. 8). In this way, occupation of CRP2 by CRP^{Mt} antagonizes activation by CRP^{Mt} bound at CRP1 resulting in inhibition of *whiB1* transcription. Because the concentration of cAMP in *M. tuberculosis* increases during infection of macrophages (5, 7), this suggests that *whiB1* might be expressed transiently during infection. Although the available microarray datasets (50, 51) do not suggest that *whiB1* expression responds transiently at the time points sampled, this study indicates that the possibility that *whiB1* is transiently expressed during infection should be tested by obtaining high resolution long time course gene expression data to determine the significance of any such transient expression for *M. tuberculosis* pathogenesis.

Acknowledgments—We thank Professor S. J. W. Busby (University of Birmingham) for the gift of the CCgalΔ4 plasmid and Luc Gaudreau and Jocelyn Beaucher (Université de Sherbrooke, Canada) for advice on RNAP purification and for a control template for in vitro transcription assays.

REFERENCES

1. Dye, C., Scheele, S., Dolin, P., Pathania, V., and Raviglione, M. C. (1999) *J. Am. Med. Assoc.* **282,** 677–686
2. Russell, D. G. (2001) *Nat. Rev. Mol. Cell Biol.* **2,** 569–577
3. Stewart, G. R., Robertson, B. D., and Young, D. B. (2003) *Nat. Rev. Microbiol.* **1,** 97–105
4. Cole, S. T., Brosch, R., Parkhill, J., Garnier, T., Churcher, C., Harris, D., Gordon, S. V., Eiglmeier, K., Gas, S., Barry, C. E., 3rd, Tekaia, F., Badcock, K., Basham, D., Brown, D., Chillingworth, T., Connor, R., Davies, R., Devlin, K., Feltwell, T., Gentles, S., Hamlin, N., Holroyd, S., Hornsby, T., Jagels, K., Krogh, A., McLean, J., Moule, S., Murphy, L., Oliver, K., Osborne, J., Quail, M. A., Rajandream, M. A., Rogers, J., Rutter, S., Seeger, K., Skelton, J., Squares, R., Squares, S., Sulston, J. E., Taylor, K., Whitehead, S., and Barrell, B. G. (1998) *Nature* **393,** 537–544
5. Agarwal, N., Lamichhane, G., Gupta, R., Nolan, S., and Bishai, W. R. (2009) *Nature* **460,** 98–102
6. Lowrie, D. B., Jackett, P. S., and Ratcliffe, N. A. (1975) *Nature* **254,** 600–602
7. Bai, G., Schaak, D. D., and McDonough, K. A. (2009) *FEMS Immunol. Med. Microbiol.* **55,** 68–73
8. Gazdik, M. A., and McDonough, K. A. (2005) *J. Bacteriol.* **187,** 2681–2692
9. Busby, S., and Kolb, A. (1996) in *Regulation of Gene Expression in Escherichia coli.* (Lin, E. C., and Lynch, A. S., eds) pp. 255–279, R. G. Landes Co., Austin, TX
10. Busby, S., and Ebright, R. E. (1999) *J. Mol. Biol.* **293,** 199–213
11. Grainger, D. C., Hurd, D., Harrison, M., Holdstock, J., and Busby, S. J. (2005) *Proc. Natl. Acad. Sci. U.S.A.* **102,** 17693–17698
12. Kirin, E., Sismeiro, O., Danchin, A., and Bertin, P. N. (2002) *Microbiology* **148,** 1553–1559
13. Berg, O. G., and von Hippel, P. H. (1988) *J. Mol. Biol.* **200,** 709–723
14. Browning, D. F., and Busby, S. J. (2004) *Nat. Rev. Microbiol.* **2,** 57–65
15. Bai, G., McCue, L. A., and McDonough, K. A. (2005) *J. Bacteriol.* **187,** 7795–7804
16. Rickman, L., Scott, C., Hunt, D. M., Hutchinson, T., Menéndez, M. C., Whalan, R., Hinds, J., Colston, M. J., Green, J., and Buxton, R. S. (2005) *Mol. Microbiol.* **56,** 1274–1286
17. Agarwal, N., Raghunand, T. R., and Bishai, W. R. (2006) *Microbiology* **152,** 2749–2756
18. Spreadbury, C. L., Pallen, M. J., Overton, T., Behr, M. A., Mostowy, S., Spiro, S., Busby, S. J., and Cole, J. A. (2005) *Microbiology* **151,** 547–556
19. Bai, G., Gazdik, M. A., Schaak, D. D., and McDonough, K. A. (2007) *Infect. Immun.* **75,** 5509–5517
20. Hunt, D. M., Saldanha, J. W., Brennan, J. F., Benjamin, P., Strom, M., Cole, J. A., Spreadbury, C. L., and Buxton, R. S. (2008) *Infect. Immun.* **76,** 2227–2234
21. Mukamolova, G. V., Turapov, O. A., Young, D. I., Kaprelyants, A. S., Kell,

D. S., and Young, M. (2002) *Mol. Microbiol.* **46,** 623–635
22. den Hengst, C. D., and Buttner, M. J. (2008) *Biochim. Biophys. Acta* **1780,** 1201–1216
23. Jakimowicz, P., Cheesman, M. R., Bishai, W. R., Chater, K. F., Thomson, A. J., and Buttner, M. J. (2005) *J. Biol. Chem.* **280,** 8309–8315
24. Alam, M. S., Garg, S. K., and Agrawal, P. (2009) *FEBS J.* **276,** 76–93
25. Singh, A., Crossman, D. K., Mai, D., Guidry, L., Voskuil, M. I., Renfrow, M. B., and Steyn, A. J. (2009) *PLoS Pathogens* **8,** e1000545
26. Soliveri, J. A., Gomez, J., Bishai, W. R., and Chater, K. F. (2000) *Microbiology* **146,** 333–343
27. Takahashi, M., Blazy, B., and Baudras, A. (1989) *J. Mol. Biol.* **207,** 783–796
28. Casadaban, M. J., and Cohen, S. N. (1980) *J. Mol. Biol.* **138,** 179–207
29. Busby, S., Kotlarz, D., and Buc, H. (1983) *J. Mol. Biol.* **167,** 259–274
30. Kubica, G. P., Kim, T. H., and Dunbar, F. P. (1972) *Int. J. Syst. Bacteriol.* **22,** 99–106
31. Snapper, S. B., Melton, R. E., Mustafa, S., Kieser, T., and Jacobs, W. R., Jr. (1990) *Mol. Microbiol.* **4,** 1911–1919
32. Lodge, J., Williams, R., Bell, A., Chan, B., and Busby, S. (1990) *FEMS Microbiol. Lett.* **67,** 221–225
33. Marsh, P. (1986) *Nucleic Acids Res.* **14,** 3603
34. Bell, A., Gaston, K., Williams, R., Chapman, K., Kolb, A., Buc, H., Minchin, S., Williams, J., and Busby, S. (1990) *Nucleic Acids Res.* **18,** 7243–7250
35. Papavinasasundaram, K. G., Anderson, C., Brooks, P. C., Thomas, N. A., Movahedzadeh, F., Jenner, P. J., Colston, M. J., and Davis, E. O. (2001) *Microbiology* **147,** 3271–3279
36. Sambrook, J. W., and Russell, D. W. (2001) *Molecular Cloning: A Laboratory Manual,* 3rd Ed., Cold Spring Harbor Laboratory Press, Cold Spring Harbor, NY
37. Wiseman, T., Williston, S., Brandts, J. F., and Lin, L. N. (1989) *Anal. Biochem.* **179,** 131–137
38. Miller, J. H. (1972) *Experiments in Molecular Genetics,* pp. 352–355, Cold Spring Harbor Laboratory Press, Cold Spring Harbor, NY
39. Maxam, A. M., and Gilbert, W. (1980) *Methods Enzymol.* **65,** 499–560
40. Beaucher, J., Rodrigue, S., Jaques, P. E., Smith, I., Brzezinski, R., and Gaudreau, L. (2002) *Mol. Microbiol.* **45,** 1527–1540
41. Akter, Y., Tundup, S., and Hasnain, S. E. (2007) *Int. J. Med. Microbiol.* **297,** 451–457
42. Angulo, J., and Krakow, J. S. (1986) *J. Biol. Chem.* **262,** 11315–11319
43. Reddy, M. C., Palaninathan, S. K., Bruning, J. B., Thurman, C., Smith, D., and Sacchettini, J. C. (2009) *J. Biol. Chem.* **284,** 36581–36591
44. Gorshkova, I., Moore, J. L., McKenney, K. H., and Schwarz, F. P. (1995) *J. Biol. Chem.* **270,** 21679–21683
45. Popovych, N., Tseng, S. R., Tonelli, M., Ebright, R. H., and Kalodimos, C. G. (2009) *Proc. Natl. Acad. Sci. U.S.A.* **106,** 6927–6932
46. Weber, I. T., and Steitz, T. A. (1987) *J. Mol. Biol.* **198,** 311–326
47. Passner, J. M., and Steitz, T. A. (1997) *Proc. Natl. Acad. Sci. U.S.A.* **94,** 2843–2847
48. Moore, J. L., Gorshkova, I. I., Brown, J. W., McKenney, K. H., and Schwarz, F. P. (1996) *J. Biol. Chem.* **271,** 21273–21278
49. Padh, H., and Venkitasubramanian, T. A. (1976) *Microbios* **16,** 183–189
50. Rohde, K. H., Abramovich, R. B., and Russell, D. G. (2007) *Cell Host Microbe* **2,** 352–364
51. Schnappinger, D., Ehrt, S., Voskuil, M. I., Liu, Y., Mangan, J. A., Monahan, I. M., Dolganov, G., Efron, B., Butcher, P. D., Nathan, C., and Schoolnik, G. K. (2003) *J. Exp. Med.* **198,** 693–704